Distribution Tail Approximation of Performance Function Via Tail Moment-Based Squared Normal Distribution

Haoran Yu[1,2,*]
[1]*State Key Laboratory of Bridge Safety and Resilience (Beijing), Beijing University of Technology, Beijing, China*
[2]*Key Laboratory of Urban Security and Disaster Engineering of Ministry of Education, Beijing University of Technology, Beijing, China*
**Corresponding Author*

Abstract: The probability distribution of the performance function serves as an essential tool for quantifying the uncertainty of structural responses. Traditional methods can construct the main body of the probability distribution but often fail to effectively capture information from the tail region, or require a considerable computational cost. Since the probability density estimation in the tail region requires particular attention, the accurate reconstruction of this region is particularly important. To address this challenge, a new method based on the squared normal distribution is proposed, in which the shape parameters are determined through the first three tail moments. As the information used for tail moment computation is extracted from the tail region corresponding to the design threshold, the final distribution achieves higher accuracy in the target tail region. Furthermore, the proposed method is applied to several different examples involving a simple performance function, a strongly nonlinear function and complex examples characterized by implicit relationships, and high dimensionality, demonstrating its superior accuracy and efficiency of the distribution tail approximation.

Keywords: Tail Moment; Squared Normal Distribution; Tail Fitting; Structural Reliability Assessment

1. Introduction

During the service life of engineering structures, various sources of uncertainty are inevitably encountered, including material variability, geometric imperfections, and environmental or loading effects. These uncertainties cause structural responses to exhibit significant randomness, which can be characterized quantitatively through the construction of the performance function. It is essential to determine the probability distribution of the performance function for a comprehensive understanding of the statistical behavior of structural responses. Since aspects such as reliability assessment [1] and design optimization [2] typically focus on the distribution tail region of the performance function, accurate reconstruction of this region is of great importance. To this end, a variety of analytical approaches have been proposed and developed, including numerical integration techniques, surrogate modeling approaches, simulation-based methods and others.

Numerical integration methods are commonly employed to indirectly reconstruct the probability density function of the performance function. Among these, the moment-based approach [3,4] has been extensively studied, which constructs the unknown distribution through the statistical moments of the performance function. This approach first assumes that the probability distribution of the performance function follows a certain probabilistic model, and then estimates the distribution parameters using low-order statistical moments (typically the first three or four moments). To accurately estimate the moments of the performance function, various moment estimation techniques have been proposed, including point estimation methods [5,6], cubature formulation method [7,8], univariate dimension reduction method (UDRM) [9], bivariate dimension reduction method (BDRM) [10,11], sparse grid integration method [12], and low-discrepancy sequences. In this process, a variety of flexible distribution models can be adopted, such as the lognormal distribution (LND) [13], the three-parameter gamma distribution [14], shifted lognormal distribution [15], squared normal distribution (SND) [16], cubed normal distribution (CND) [17], generalized lambda distribution (GLD) [18], shifted generalized lognormal distribution (SGLD) [19], Pearson system [20], Hermite model [21], saddle point approximation [22,23], and maximum entropy distributions based on integer-order moments [24]. The use of very high-order moments (fifth or sixth order) [25] is a natural extension of the moment-based approach. However, obtaining such high-order moments poses a significant challenge. In addition, the introduction of L-moments [26,27] and fractional-order moments [28,29] provides further flexibility to the method. Nevertheless, limitations of moment-based methods remain, particularly in accurately approximating the light-tail region. In recent years, several nonparametric distribution approaches have been developed to evaluate complex distributions. The method based on the improved Mellin transform [30], as well as the approach combining the maximum entropy principle with B-splines [31-37], have demonstrated their inherent strong applicability. However, nonparametric distributions are generally sensitive to sparse samples in the tail region and perform poorly in predicting tail probabilities.

Simulation-based methods are widely used due to their generality and intuitive nature. Monte Carlo Simulation (MCS), as a fundamental approach, generates samples of the performance function by randomly sampling the input random variables, enabling estimation of system responses or failure probabilities. However, accurately evaluating rare events requires extremely high computational cost, making MCS often impractical for direct engineering applications. Consequently, MCS is commonly employed as a benchmark to assess the accuracy and efficiency of alternative methods. To mitigate this limitation, various advanced sampling techniques have been developed, including directional sampling (DS) [38,39], importance sampling (IS) [40,41], Latin Hypercube Sampling (LHS) [42,43], and subset simulation (SS) [44-46]. Although these methods can improve computational efficiency, balancing accuracy and cost remains challenging. Moreover, the lack of the explicit PDF is another inherent limitation, as these approaches are primarily suited for estimating single probabilities (e.g., structural failure probability). For extreme events associated with lower threshold values, these methods struggle to extrapolate probabilities reliably, thereby constraining their applicability in certain engineering scenarios.

In a broad range of practical engineering scenarios, structural responses may involve complex performance functions. In such cases, uncertainty quantification can only be indirectly obtained through a limited number of stochastic evaluation results. Due to constraints on computational cost and sample size, how to extract effective statistical information from limited random samples and accordingly recover distribution characteristics (especially tail behavior) becomes a key issue. From this perspective, random sample-based statistical inference methods have a clear practical demand, which has also promoted the development and application of post-processing methods. These methods generally perform a limited number of simulations first, and then analyzing the simulation outputs. In this way, the probability distribution can be efficiently estimated using only a limited number of samples, and the efficiency is largely insensitive to the dimensionality of the random variables or the complexity of the performance functions. Post-processing methods have attracted increasing attention in recent years and have been successfully applied to stochastic dynamic problems. Among these, it is worth noting a class of methods that specifically treat and model only the distribution tail region. The generalized Pareto distribution (GPD) [47] based on maximum likelihood estimation is only suitable for heavier tails. Tail-modification models based on the least squares method include both polynomial and exponential forms [48,49]. However, the preliminary processing using kernel density estimation (KDE) may distort the original shape of the curve of cumulative distribution function (CDF), which introduces additional bias. Subsequently, Weng et al. proposed a Bayesian-based truncated SGLD [50]. Although this method performs well for heavier tail distributions, its applicability to narrow-tailed distributions remains to be further verified. To improve the approximation of distribution tail regions, this paper proposes a tail moment-based squared normal distribution. The proposed method does not impose any assumptions on the tail shape and therefore exhibits strong adaptability in handling different types of tail behaviors. Additionally, the method has a compact formulation and facilitates practical implementation. The introduction of tail moments helps mitigate the influence of the full distribution and improves the efficiency of extracting and utilizing tail statistical information.

The specific framework of this paper is as follows: Section 2 presents the problem formulation. Section 3 introduces the tail moment-based squared normal distribution. Section 4 demonstrates the application of the proposed method, including the tail-region fitting of a simple performance function, a strongly nonlinear function, an implicit performance function and a high-dimensional performance function. Section 5 summarizes the findings of this study.

2. Problem Description

Consider a structure characterized by an n-dimensional input random variables $\boldsymbol{X}=[X_1,X_2,\dots X_n]^T$. The performance function of the structure can be expressed as

$$Z=g(X) \tag{1}$$

where Z represents a new random variable obtained by mapping the uncertainty of the input random variable $\boldsymbol{X}$ through the performance function $g(\cdot)$.

In many practical engineering scenarios, particular attention is often devoted to the tail region of the distribution, since extreme events (e.g., structural failures) typically occur in this region (e.g., $<10^{-1}$). Without loss of generality, this study focuses on the left tail region of the probability distribution of the performance function, whose cumulative distribution function (CDF) can be expressed as

$$F_Z(z)=p(Z\leq z)=p[g(X)\leq z]=\int_{g(X)\leq z} f_X(x)dx \tag{2}$$

where $f_X(\cdot)$ represents the joint PDF of the input random variables $\boldsymbol{X}$.

By differentiating Eq. (2) with respect to z, the probability density function (PDF) of the random variable Z can be obtained as

$$f_Z(z)=dF_Z(z)/dz \tag{3}$$

Eqs. (2)-(3) typically lack a closed-form analytical solution. Although various numerical techniques have been developed to address this issue, substantial challenges still remain. On one hand, when the performance function involves high-dimensional random variables or computationally intensive models (e.g., finite element models or nonlinear dynamic response analyses), the computational process becomes exceedingly complex and time-consuming, often rendering the analysis infeasible within acceptable computational resources. On the other hand, accurately estimating the probability of extreme events in the tail region remains a long-standing challenge. Consequently, achieving substantial improvements in computational efficiency while maintaining high accuracy remains a critical research direction that warrants further investigation.

3. Proposed tail Approximation Method

3.1 Sample-based Tail Moment Estimation

Central moments are only sensitive to the one-sided tail, and the fitting error increases as z approaches the farther tail region. To mitigate this effect, tail moments are employed in this study to construct the distribution of Z. For the variable Z, its left tail moments are defined as

$$\mu_L=\int_{-\infty}^{\delta} x f_L(x)\mathrm{d}x \tag{4a}$$

$$\sigma_L^2=\int_{-\infty}^{\delta} (x-\mu_L)^2 f_L(x)\mathrm{d}x \tag{4b}$$

$$\alpha_{Lr}\sigma_L^r=\int_{-\infty}^{\delta} (x-\mu_L)^r f_L(x)\mathrm{d}x \quad (r\geq 3) \tag{4c}$$

where μ_L denotes the first-order tail moment; σ_L denotes the second-order tail moment; α_{Lr} denotes the r-th standardized tail moment. δ represents the threshold of the tail moments. In general, $\delta=F_z(0.5)$; L represents the transition variable formed in this process, and $f_Z(x)$ is the distribution of L, i.e., the conditional distribution of Z $(f_L(x)=f_Z(x)/F_Z(\delta))$.

The above tail moment expressions can be directly evaluated based on samples. For example, the required samples may be efficiently generated using the Latin Hypercube Sampling (LHS) method. Compared with conventional Monte Carlo simulation (MCS), LHS generally exhibits better space-filling properties and higher sampling efficiency. Assume that a set of samples has been generated by LHS and sorted in ascending order as: $z_1,z_2,\dots,z_i,\dots,z_N$, N is total sample size. The threshold δ can be readily determined. Subsequently, the corresponding tail moments are calculated by selecting the samples falling within the target tail region. The first three tail moments can be expressed as

$$\mu_L=\frac{1}{N_L}\sum_{j=1}^{N_L} z_j \tag{5a}$$

$$\sigma_L^2=\frac{1}{N_L}\sum_{j=1}^{N_L}\left(z_j-\mu_L\right)^2 \tag{5b}$$

$$\alpha_{Lr}=\frac{1}{N_L}\sum_{j=1}^{N_L}\left(\frac{z_j-\mu_L}{\sigma_L}\right)^3 \tag{5c}$$

where N_L denotes the number of samples in the target tail region; z_j represents the samples from the target tail region, z_j should satisfy $z_j \geq \delta$.

3.2 Squared Normal Distribution

Furthermore, by using the input information, the distribution of L can be directly constructed based on the sample-based tail moments. Once L is obtained, it can be directly mapped back to the original variable Z. In this study, The squared normal distribution combined with the first three tail moments (μ_L, σ_L and α_{L3}) is adopted to obtain the distribution of L. This distribution is constructed based on the following transformation

$$(L-\mu_L)/\sigma_L = S^{-1}(U) = a + bU + cU^2 \quad (6)$$

where $S^{-1}(\cdot)$ denotes the transformation function; U represents a standard normal variable; a b and c are the shape parameters.

The three parameters a b and c in Eq. (6) are determined by equating the first three moments on both sides of the equations, which finally can be specifically expressed as:

$$c = sign(\alpha_{L3})\sqrt{2}\cos\left(\frac{\pi+|\theta|}{3}\right) \quad (7a)$$

$$a = -c \quad (7b)$$

$$b = \sqrt{1-c^2} \quad (7c)$$

where $\theta = \tan^{-1}\left(\frac{\sqrt{8-\alpha_{L3}}^{2}}{\alpha_{L3}}\right)$.

The final CDF and PDF of Z can be expressed as

$$F_Z(z) = F_Z(\delta)\Phi\left([\sqrt{b^2-4c(a-z_s)}-b]/2c\right) \quad (8)$$

$$f_Z(z) = F_Z(\delta)\frac{\phi\left([\sqrt{b^2-4c(a-z_s)}-b]/2c\right)}{\sigma_L\sqrt{b^2-4c(a-z_s)}} \quad (9)$$

where $z_s = (z-\mu_L)/\sigma_L$; $\Phi(\cdot)$ and $\phi(\cdot)$ are the CDF and PDF of the standard normal distribution.

To make the Eq. (8) and Eq. (9) operable, it need be satisfied that for $c \geq 0$, $a - b^2/4c \leq z_s \leq \delta$; for $c < 0$, $z_s \leq \min\left(a - b^2/4c, \delta\right)$.

4. Numerical Illustrations

4.1. Two-dimensional performance function

A simple two-dimensional performance function is employed, as referenced in [51]. It can be formulated as Eq. (10). This example is used to investigate the performance of the proposed method under different sample sizes and to determine the final sample size adopted in this study.

$$g(X) = \frac{5}{2} - \frac{1}{216}(X_1+X_2-20)^4 - \frac{33}{140}(X_1+X_2) \quad (10)$$

where $X_1 \sim N(0,1)$, $X_2 \sim N(0,1)$

This example is mainly used to investigate the influence of sample size on the stability of tail moments. To this end, sample sizes ranging from 200 to 1000 are considered, with an increment of 200 samples at each step. As shown in Fig. 1, it can be observed that when the sample size is small, not only the third-order tail moment exhibits significant instability, but the first- and second-order tail moments also show considerable fluctuations (Table 1). As the sample size increases, the instability of the tail moments gradually decreases. Furthermore, Fig. 2 indicates that the sample size of 1000 can provide a sufficiently good fitting performance. Therefore, the recommended sample size can be set as 1000.

Table 1. First Three Tail Moments Under Different Samples for Case 1

Sample Size	μ_L	σ_L	α_{L3}
200	-942.2643	191.7539	-1.8014
400	-922.8246	147.5573	-1.2813
600	-923.5075	161.7629	-1.4176
800	-926.4528	160.3804	-1.3499
1000	-926.6003	155.9351	-1.3602

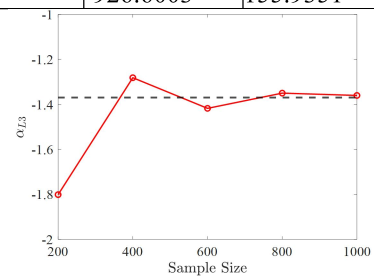

Figure 1. Dependence Relationship of the Third-order Tail Moment on Sample Size

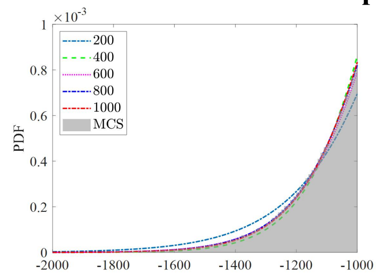

(a) PDF

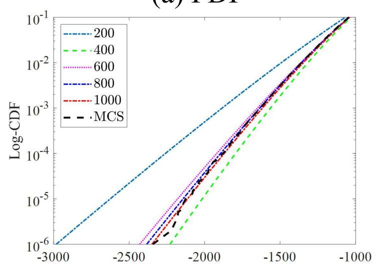

(b) CDF

Figure 2. Distribution Tail of Case 1 under Different Samples

4.2 Strongly Nonlinear Performance Function

In the third example, a strongly nonlinear performance function is studied from [52]. The performance function is expressed as Eq. (11), and the basic information of the random variables is listed in Table 2.

$$g(X) = 5 - \sum_{i=1}^{n} X_i - 20X_1^2X_2^2 - \sum_{i=1}^{n-2} X_{i+1}^2 X_{i+2}^2 + \sum_{i=1}^{n} \sin(X_i) exp(X_i - 2) \quad (11)$$

Table 2. Basic Information of Random Variables for Example 2

random variable	distribution	μ	σ
X_1	Normal	1.00	0.10
X_2	Normal	1.00	0.20
X_3	Gumbel	1.00	0.10
X_4	Weibull	0.50	0.10
X_5~X_6	Lognormal	2.00	0.10
X_7~X_{10}	Normal	1.00	0.10

In this case, the central moment-based squared normal (CM-SN) method is selected for comparative analysis. Both methods use the same set of samples. As shown in Fig. 3(b), the CM-SN method deviates from the MCS results at the order of 10^{-2} in the CDF. In contrast, by incorporating tail moments, the proposed method improves the fitting accuracy in the tail region. Such accuracy can be maintained down to approximately the order of 10^{-4}.

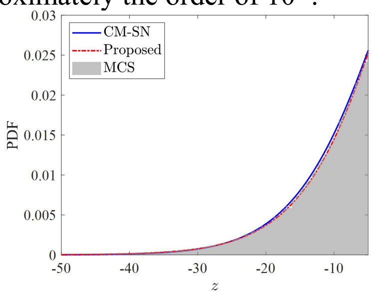

(a) PDF

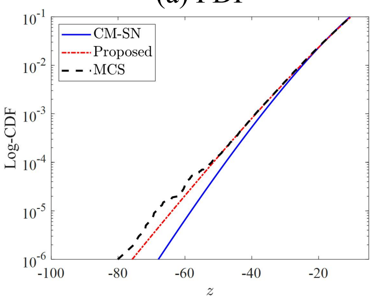

(b) CDF

Figure 3. Distribution Tail of Case 2

4.3 Implicit Performance Function

The third example involves a 12-story, three-bay linear frame structure, as illustrated in the Fig. 4, adapted from [53]. In this case, the cross-sectional areas and horizontal loads are considered as independent random variables, with their fundamental statistical properties summarized in the Table 3. The moment of inertia of each section is denoted as $I_i = \lambda_1 A_i^2 \cdot (\lambda_1 = \lambda_2 = \lambda_3 = 0.08, \cdot \lambda_4 = 0.27, \lambda_5 = 0.2)$ and the elastic modulus E is treated as deterministic, $E = 2.0 \times 10^7 kN/m^2$. The element types are shown in Fig. 4. The quantity of interest is the probability that the horizontal displacement at node T (u_T) exceeds the limiting value $[u] = H/500 = 0.096m$, where H denotes the total height of the 12-story frame. The corresponding performance function is expressed as

$$g(X)=0.096-u_T(X) \quad (12)$$

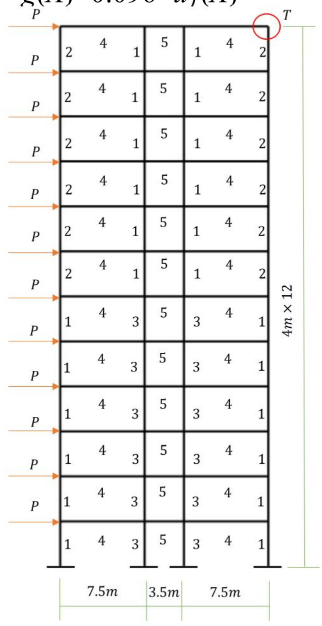

Figure 4. Simplified Model of 12-Storey Frame Structure

Table 3. Basic Information of Random Variables for Example 4

random variable	distribution	μ	σ
A_1	Lognormal	0.25	0.10
A_2	Lognormal	0.16	0.10
A_3	Lognormal	0.36	0.10
A_4	Lognormal	0.20	0.10
A_5	Lognormal	0.15	0.10
P	Gumbel	30.00	0.15

In this case, the CM-SN method is employed for comparative analysis. Fig. 5 illustrates the PDF and CDF fitting results. The performance of the CM-SN method deteriorates rapidly starting from approximately the order of 10^{-2}. In contrast, the proposed method achieves an approximation accuracy up to the order of 10^{-5}. Moreover, a comparison of the failure probability estimates in Table 4 further demonstrates that the proposed method provides higher accuracy than the original CM-SN method.

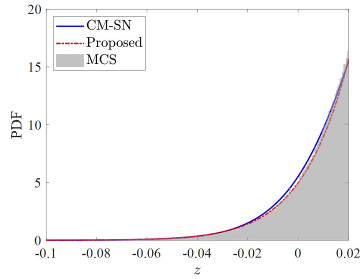

(a) PDF

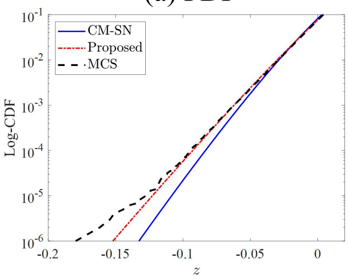

(b) CDF

Figure 5. Distribution Tail of Case 3

Table 4. Failure Probability Estimation Results for Case 3

	CM-SN	Proposed	MCS
p_f	0.0824	0.0770	0.0759
error	8.5639%	1.4493%	

4.4 High-Dimensional Performance Function

The fourth example [54] concerns a thin, solid square plate commonly used in the field of stochastic finite element analysis, aiming to demonstrate the applicability of the proposed method to high-dimensional stochastic input problems. As illustrated in Fig. 6, the lower edge of the plate is fixed, while the opposite edge is subjected to a uniform tensile load. The plate dimensions are set as $L_X = 1$, $L_Y = 1$ and $t = 1$. The Poisson's ratio of the material is taken as 0. The plate is discretized into 16 four-node quadrilateral finite elements. The uniformly distributed load q is deterministic with a unit magnitude. The Young's modulus E is modeled as a two-dimensional Gaussian random field with a known mean μ_E and standard deviation σ_E, expressed as follows:

$$E(x,y) = \mu_E[1 + \alpha(x,y)] \tag{13}$$

where $\alpha(x,y)$ represents a zero-mean Gaussian random field characterized by the following autocovariance function:

$$C(x,y)=\sigma_E^2 \exp\left(-\frac{|x_1-y_1|}{b_1}-\frac{|x_2-y_2|}{b_2}\right) \tag{14}$$

where b_1 and b_2 are the correlation length parameters. The parameters involved are specified as μ_E=1, σ_E=0.1, and b_1=b_2=0.5. By employing the Karhunen–Loève (K–L) expansion, the random field can be approximated by a truncated series of the following form as

$$\alpha(x,y) \approx \sum_{i=1}^{n} \sqrt{\lambda_i}\,\theta_i \Omega(x,y) \tag{15}$$

where n denotes the number of truncated terms; λ and Ω are the eigenvalues and eigenfunctions of the autocovariance function, respectively; and θ are independent standard normal random variables. In this study, a total of 150 truncated terms (n=150) are employed in the K–L expansion.

The final performance function is defined as follows:

$$g(X)=\Delta_b-\Delta_{23} \tag{16}$$

where Δ_{23} is the vertical displacement at node 23, and Δ_b is a deterministic threshold value set to 1.25.

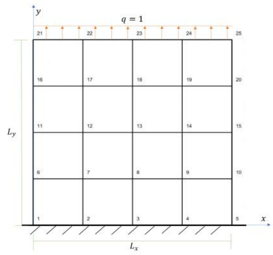

Figure 6. Simplified Model of Thin Solid Square Plate

In this high-dimensional stochastic input case, a comparative analysis is conducted between the CM-SN method and the proposed method. As shown in the CDF curves in Fig. 7(b), using the same samples, the CM-SN method remains effective only up to approximately the order of 10^{-2}, beyond which it exhibits a pronounced underestimation of probabilities. In contrast, the proposed method maintains good agreement with the MCS results over the entire CDF range, demonstrating the accurate reconstruction of the distribution in the tail region. Furthermore, in Table 5, the failure probability is on the order of 10^{-4}, the CM-SN method shows significant deviation. In contrast, the proposed method yields results that are closely consistent with those obtained from MCS.

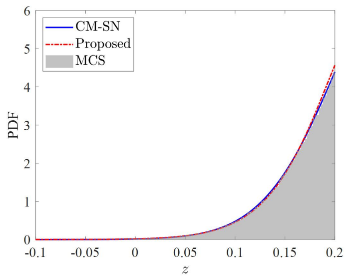

(a) PDF

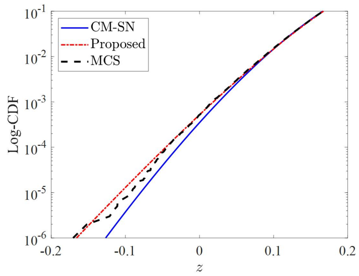

(b) CDF

Figure 7. Distribution Tail of Case 4

Table 5. Failure Probability Estimation Results for Case 4

	CM-SN	Proposed	MCS
p_f	3.4821×10^{-4}	5.19×10^{-4}	5.18×10^{-4}
error	32.7780%	0.1931%	

5. Conclusion

In this study, a novel probability density estimation approach is developed, which provides the robust and accurate evaluation of the distribution tail regions of interest. The principal contributions of this work can be summarized as follows:

(1) A tail moment-based squared normal distribution is developed to specifically characterize the tail region of interest. The proposed method offers high flexibility without imposing any assumptions on the tail behaviors of a distribution. This method overcomes the limitation of conventional central moment-based approaches, which are typically sensitive only to one-sided tail region. Moreover, it improves the accuracy of probability estimation.

(2) The proposed method attains the same level of efficiency as over one hundred thousand MCS runs with only a thousand samples, leading to a substantial reduction in computational cost. The design threshold enables more samples to participate in the evaluation of the first three tail moments, thereby maintaining the relative stability of the assessment results.

(3) In this study, the wide applicability of the method is systematically validated through representative cases characterized by strong nonlinearity, implicit functional relationships, and high-dimensional random inputs. The results demonstrate that the proposed method can achieve accuracy comparable to that of the MCS, while requiring significantly less computational effort, highlighting its strong potential for efficient and reliable estimation of rare event probabilities in complex engineering systems.

Future research can be directed toward two main aspects: (1) integrating or developing more robust sampling strategies to enhance the stability of tail moment estimation; (2) investigating and utilizing higher-order tail moments and reconsider the design threshold to enable the acquisition of extremely small probabilities and flexible construction of distribution tails with diverse forms.

References

[1] Xu J, Song J, Yu Q, et al. Generalized distribution reconstruction based on the inversion of characteristic function curve for structural reliability analysis. Reliab Eng Syst Saf 2023; 229: 108768.

[2] Jiang Y, Zhang X, Beer M, et al. An efficient method for reliability-based design optimization of structures under random excitation by mapping between reliability and operator norm. Reliab Eng Syst Saf 2024; 245: 109972.

[3] Zhao YG, Ono T. Moment methods for structural reliability. Struct Saf 2001; 23(1): 47-75.

[4] Zhao YG, Lu ZH. Structural reliability: Approaches from perspectives of statistical moments. Wiley 2021.

[5] Zhao YG, Ono T. New point estimates for probability moments. J Eng Mech 2000; 126(4): 433-436.

[6] Cai CH, Lu ZH, Xu J, et al. Efficient algorithm for evaluation of statistical moments of performance functions. J Eng Mech 2019; 145(1): 06018007.

[7] Xu J, Lu Z H. Evaluation of moments of performance functions based on efficient cubature formulation. J Eng Mech 2017; 143(8): 06017007.

[8] Zhang D, Shen S, Jiang C, et al. An advanced mixed-degree cubature formula for reliability analysis. Comput Methods Appl Mech Eng 2022; 400: 115521.

[9] Rahman S, Xu H. A univariate dimension-reduction method for multi-dimensional integration in stochastic mechanics. Probabilistic Eng Mech 2004; 19(4): 393-408.

[10] Huang B, Du X. Uncertainty analysis by dimension reduction integration and saddle point approximations. In: International Design Engineering Technical Conferences and Computers and Information in Engineering Conference. 2005; 4739: 1143-1152.

[11] Ding C, Xu J. An improved adaptive bivariate dimension-reduction method for efficient statistical moment and reliability evaluations. Mech Syst Signal Process 2021; 149: 107309.
[12] Wang T, Li J, Lu D, et al. A point mapping strategy-based sparse grid integration method for statistical moments estimation and structural reliability analysis. Comput Methods Appl Mech Eng 2024; 430: 117238.
[13] Famoye F. Continuous univariate distributions, volume 1. 1995.
[14]Zhao YG, Ang AHS. Three-parameter gamma distribution and its significance in structural reliability. Comput Struct Eng Int J 2002; 2(1): 1-10.
[15] Tichý M. First-order third-moment reliability method. Struct Saf 1994; 16(3): 189-200.
[16] Zhao YG, Ono T, Idota H, et al. A three-parameter distribution used for structural reliability evaluation. J Struct Constr Eng AIJ 2001; 66(546): 31-38.
[17] Zhao YG, Zhang XY, Lu ZH. A flexible distribution and its application in reliability engineering. Reliab Eng Syst Saf 2018; 176: 1–12.
[18] Zhao YG, Lu ZH, Ono T. 4p-Lambda distribution and its applications to structural reliability assessment. J Struct Constr Eng AIJ 2006; 71(604): 47–54.
[19] Low YM. A new distribution for fitting four moments and its applications to reliability analysis. Struct Saf 2013; 42: 12-25.
[20] Pearson KX. Contributions to the mathematical theory of evolution. II. Skew variation in homogeneous material. Philos Trans R Soc Lond A 1895; 186: 343-414.
[21] Winterstein SR. Nonlinear vibration models for extremes and fatigue. J Eng Mech 1988; 114(10): 1772–1790.
[22] Daniels HE. Saddle point approximations in statistics. Ann Math Stat 1954; 25(4): 631–650.
[23] Zhou D, Pan E, Zhang X, et al. Dynamic model-based saddle-point approximation for reliability and reliability-based sensitivity analysis. Reliab Eng Syst Saf 2020; 201: 106972.
[24] Jaynes E T. Information theory and statistical mechanics. Phys Rev 1957; 106(4): 620–630.
[25] Zhao YG, Wang T, Ji X, et al. Quartic Hermite polynomial model-based translation method for extreme wind load estimation. J Wind Eng Ind Aerodyn 2024; 245: 105653.
[26] Tong MN, Zhao YG, Zhao Z. Simulating strongly non-Gaussian and non-stationary processes using Karhunen–Loève expansion and L-moments-based Hermite polynomial model. Mech Syst Signal Process 2021; 160: 107953.
[27] Tong MN, Zhao YG, Lu ZH. A flexible distribution based on L-moments and its application in structural reliability. ASCE-ASME J Risk Uncertain Eng Syst B 2025; 11(4): 041202.
[28] Xie W, Huang P, Gu M. A maximum entropy model with fractional moments for probability density function estimation of wind pressures on low-rise building. J Wind Eng Ind Aerodyn 2021; 208: 104461.
[29] Wang L, Wang T, Dong Y, et al. Structural reliability analysis based on fractional moments-based iterative maximum entropy method and multiplicative exact dimension reduction integration method. Reliab Eng Syst Saf 2025; 111344.
[30] Xu J, Yu Q. Harmonic transform-based non-parametric density estimation method for forward uncertainty propagation and reliability analysis. Struct Saf 2023; 103: 102331.
[31] He W, Wang Y, Li G, et al. A novel maximum entropy method based on the B-spline theory and the low-discrepancy sequence for complex probability distribution reconstruction. Reliab Eng Syst Saf 2024; 243: 109909.
[32] Xie B, Peng C, Wang Y. Combined relevance vector machine technique and subset simulation importance sampling for structural reliability. Applied Mathematical Modelling 2023; 113: 129-143.
[33] Echard B, Gayton N, Lemaire M. AK-MCS: an active learning reliability method combining Kriging and Monte Carlo simulation. Structural Safety 2011; 33(2): 145-154.
[34] Weng Y Y, Liu T, Zhang X Y, et al. Probability density estimation of polynomial chaos and its application in structural reliability analysis. Reliability Eng & Syst Saf 2025; 253: 110537.
[35] Echard B, Gayton N, Lemaire M, et al. A combined importance sampling and kriging reliability method for small failure

probabilities with time-demanding numerical models. Reliability Eng & Syst Saf 2013; 111: 232-240.

[36] Zhao H, Yue Z, Liu Y, et al. An efficient reliability method combining adaptive importance sampling and Kriging metamodel. Applied Mathematical Modelling 2015; 39(7): 1853-1866.

[37] Wei X, Chang H, Feng B, et al. Hull form reliability-based robust design optimization combining polynomial chaos expansion and maximum entropy method. Applied Ocean Research 2019; 90: 101860.

[38] Melchers R E. Structural system reliability assessment using directional simulation. Struct Saf 1994; 16(1-2): 23-37.

[39] Nie J, Ellingwood B R. Directional methods for structural reliability analysis. Struct Saf 2000; 22(3): 233-249.

[40] Melchers R E. Importance sampling in structural systems. Struct Saf 1989; 6(1): 3-10.

[41] Au S K. Probabilistic failure analysis by importance sampling Markov chain simulation. J Eng Mech 2004; 130(3): 303-311.

[42] Stein M. Large sample properties of simulations using Latin hypercube sampling. Technometrics 1987; 29(2): 143-151.

[43] Shields M D, Zhang J. The generalization of Latin hypercube sampling. Reliab Eng Syst Saf 2016; 148: 96-108.

[44] Papaioannou I, Betz W, Zwirglmaier K, et al. MCMC algorithms for subset simulation. Probabilistic Eng Mech 2015; 41: 89-103.

[45] Wang Z, Broccardo M, Song J. Hamiltonian Monte Carlo methods for subset simulation in reliability analysis. Struct Saf 2019; 76: 51-67.

[46] Mestry D V, Bhowmick A R. Demystifying Monte Carlo methods in R: A guide from Metropolis–Hastings to Hamiltonian Monte Carlo with biological growth equation examples. Ecol Model 2025; 501: 110922.

[47] Grigoriu M, Samorodnitsky G. Reliability of dynamic systems in random environment by extreme value theory. Probabilist Eng Mech 2014; 38: 54–69.

[48] Xu J, Ding Z, Wang J. Extreme value distribution and small failure probabilities estimation of structures subjected to non-stationary stochastic seismic excitations. Struct Saf 2018; 70: 93–103.

[49] Weng YY, Lu ZH, Li PP, et al. Dynamic reliability analysis of structures under nonstationary stochastic excitations using tail-modified extreme value distribution. Mech Syst Signal Process 2023; 198: 110424.

[50] Weng YY, Zhang XY, Lu ZH, et al. A conditional extreme value distribution method for dynamic reliability analysis of stochastic structures. Struct Saf 2024; 106: 102398.

[51] Ghalehnovi M, Rashki M, Ameryan A. First order control variates algorithm for reliability analysis of engineering structures. Applied Mathematical Modelling 2020; 77: 829-847.

[52] Shen S, Cheng J, Liu Z, et al. Bayesian inference-assisted reliability analysis framework for robotic motion systems in future factories. Reliab Eng Syst Saf 2025; 258: 110894.

[53] Lan C, Li H, Peng J, et al. A structural reliability-based sensitivity analysis method using particles swarm optimization: relative convergence rate. J Zhejiang Univ-SCI A 2016; 17(12): 961-973.

[54] Dang C, Xu J. Unified reliability assessment for problems with low-to high-dimensional random inputs using the Laplace transform and a mixture distribution. Reliab Eng Syst Saf 2020; 204: 107124.